Malaysian Catalysis-An International Journal

Malay. Catal.Int.J Vol 2, Issue 1 (2022) 01-20

RESEARCH ARTICLE

Scrap Gold Recovery: Recycling, Fabrication and Electrochemical Characterization of Low-Cost Gold Electrode

Received 13th May 2022,
Revised 13th June 2022,
Accepted 14th June 2022

DOI: 10.22452/mcij.vol2no1.1

Corresponding author:
zithrox@gmail.com

Mohammad Al Mamun[ab*], Yasmin Abdul Wahab[a*], M. A. Motalib Hossain[a], Abu Hashem[ac], Mohd Rafie Johan[a]

[a] Nanotechnology and Catalysis Research Centre, Institute for Advanced Studies, Universiti of Malaya, 50603 Kuala Lumpur, Malaysia.
[b] Department of Chemistry, Jagannath University, Dhaka-1100, Bangladesh.
[c] Microbial Biotechnology Division, National Institute of Biotechnology, Ganakbari, Ashulia, Savar, Dhaka-1349

Abstract

As a noble metal, gold is considered the most popular material in electrocatalysis. In spite of that, this metal is a highly expensive material in the manufacture of low-cost devices. In the present work, scrap gold, produced in jewelry as waste, is introduced as a low-cost resource of gold to be recycled. A gold electrode was fabricated by connecting the tablet-shaped recycled gold with copper wire and inserting it into a polytetrafluoroethylene (PTFE) tube. The manufactured electrodes are easily renewable, modifiable with nanomaterials, and show excellent electrochemical characteristics in the presence of redox species. The fabricated bare and gold nanoparticles modified electrodes show quasi-reversible interfacial charge transfer kinetics controlled by mass-transport. The modified electrode exhibits good reproducibility with electrocatalytic activity in presence of $[Fe(CN)_6]^{4-/3-}$ redox couples. They also displayed a significantly large peak separation potential between the oxidation and reduction peaks at different scan rates. The CV (cyclic voltammetry), DPV (differential pulse voltammetry), and EIS (electrochemical impedance spectroscopic) analysis data infer that the developed recycled gold-based electrodes would be suitable not only for the development of low-cost electrocatalytic sensors devices but also for routine electroanalysis.

Keywords: scrap gold; recycling, low-cost electrode; electrochemical, characterization

1. Introduction

Gold is anticipated to play a major role as a catalyst in a variety of industrial and non-industrial applications. Due to its passive nature compared to other metals, gold (Au) has been the source of many wonderful historical goods. It is inert for many catalytic reactions because it is too noble, but it has become incredibly active when partitioned at the nanoscale [1]. Gold is utilised in a wide range of products, from high-end accessories to carefully guarded bars to tiny amounts in technological devices. Heterogeneous catalysis using gold nanoparticles has been a "hot issue" since it may be employed in a number of industrially and environmentally crucial oxidation reactions, such as sensor technologies and hydrogen fuel production [2-8], with new discoveries being made on a regular basis. In the last decade, the use of functionalized gold nanoparticles (AuNPs) for targeted sensing of particular biomolecules has become a popular research topic [4, 9]. AuNP-based sensors are expected to change the principles of sensing and recognising biomolecules. In addition to sensing [3, 10], gold nanoparticles are intriguing candidates for photothermal therapy, diagnostic, and drug delivery applications [10-13]. Due to their excellent properties such as highly resonant particle plasmons, conductivity, direct visualisation of single nanoclusters by light scattering, electrochemical properties, and colloidal AuNPs are appealing materials for many biotechnology applications. AuNPs can also easily attach to biomolecules, which makes them good candidates for transducers in sensing technologies for a wide range of bioreceptor uses [4, 14-20].

The cost of gold materials, on the other hand, is a crucial consideration in assessing the viability of its applications [21]. It is a costly material, which limits its use in various fields, despite its superb performances compare to other metals. Mining (74%), high-value gold recycling (23%), and electronic scrap (3%) are the gold pathways that satisfy the world gold supply [22]. In 2018, the overall gold supply was 4670 tons, with 23% coming from the refinement of gold-containing debris like jewellery or coins, 3% from the recovering of waste electronic equipment, and the remainder coming from freshly mined gold [23]. Gold scraps can come from a variety of sources, including waste electronic and electrical items, jewellery, used dental and orthopaedic components, spent catalysts, and so on, and come in a variety of shapes and sizes. Gold that is 'lost' throughout the production process can have a major impact on product costs and profitability. Whether gold jewellery is manufactured using conventional methods in a workshop or bulk production in a factory, scrap material, including defective jewellery, is always generated. Scrap

occurs at every stage of jewellery production, including debasing and bar production, investment casting along with defective castings and feeders, stamping with blanking processes, drilling, workbench filing, sawing, soldering, and finishing (diamond cutting, polishing, and so on) [24]. But the processing of such trace gold is difficult [25] to recover with high purity. Scrap is made up of abandoned materials from the manufacturing process as well as rejected jewellery. This might range from high to modest in terms of precious metal content. Damaged and worn products returned by consumers or purchased on the open market are likewise a high-grade gold supply, although the quality is less certain. That jewellery scrap gold could be a great low-cost source of high-quality gold recycling. Therefore, a simple and effective recycling procedure is required.

Cupellation, Miller chlorination, Wohlwill electrolysis, and the Aqua Regia process are some of the methods for recovering gold from various sources [24, 26], but all are not appropriate for the in-house small-scale refining or in a jewellery manufacture atmosphere. For example, the cupellation process needs very high temperature, it releases abundant quantities of poisonous metal oxide emissions, creating air pollution unless costly fume reduction systems (gas scrubbers) are to be set up [23]. Hence, this process is not recommended for small-scale home recycling of gold. In Miller chlorination process, it is needed extensive technical skills to run the process and have substantial health and safety allegations in work with Cl_2 gas. Consequently, this process is not suitable to small-scale refining. The Wohlwill electrolytic process is an old-fashioned, recognized procedure for the high-scale gold refining. But it is a long-time process that endures from the lock-up of gold supply in the electrolytic cell associated with the expensive gold electrode and constant power supply. As a result, it is not recommended for small-scale in-house refiners. The Aqua Regia procedure, on the other hand, is the simplest, fastest, and most robust of them all, is an efficient method for recovering gold with high purity. Furthermore, on a small-medium size, this technique is the most extensively employed by refineries and jewellers alike, and able to produce gold with a purity close to 100%, which is crucial for the electrode construction.

Gold is one of the most widely used solid metallic electrodes in the field of electroanalytical chemistry on account of its excellent electrochemical properties, the ease of surface modification by self-assembling and the inertness in the presence of almost all chemical reagents [27, 28]. Due to the extreme price of gold electrodes, the development of low-cost devices has fueled the quest for alternate methodologies and/or less expensive supplies of this metal [28, 29]. Highly pure gold is required for electrode production, which raises the electrode cost even more. The soaring

expense of gold-based electrodes has encouraged researchers to explore inexpensive sources of this noble metal, motivated by the advancement of reproducible, renewable, disposable, wearable, and low-cost sensor devices. Keeping the cost factor in mind, a group of scientists in 1997 introduced a gold micro-electrode arrays using split integrated circuit chips [29]. The electrochemical performance of those electrodes was satisfactory in terms of the uniformity of their electrode surface. But they are not satisfactory regarding the repeated use of the same electrode surface. 3 years later, Angnes et. al 2000 reported a versatile method of fabrication for gold electrodes named 'CDtrodes' employing recordable CDs as the less-expensive source of gold [28]. Those electrodes are easy to fabricate and reproducible for single use, but they are not fit for multiple uses after renewal of the same surface due to their extremely low electrode thickness. Recently, M.S.F. Santos and his co-workers reported a gold-leaf sheet, used in low-cost source of gold such as wedding candies and decorative crafts, based electrodes [30]. Those electrodes were disposable and wearable, but the reproducibility was not sufficient (the relative standard deviation or RSD was about 4%). Moreover, the renewal process of the electrode surface was not efficient as the old surface must be rejected after cutting with a sharp blade, which causes the wastage of gold. Therefore, the electrochemical performance of those reported electrodes suffers from the lack of sufficient reproducibility, multiple use, and renewability of the electrode surface, which could reduce the cost significantly. The potential reason behind those drawbacks might be the lack of adequate purity owing to their direct use of the gold-based waste materials without extraction and purification of gold from those bulk materials.

In our current study, we employed the Aqua Regia process to recycle gold from high-grade jewellery trash gold, and this purified gold was used to fabricate a low-cost gold electrode (AuE) to minimize those limitations. The performance of the manufactured AuE surface was investigated using several electrochemical techniques such as CV, DPV and EIS as those techniques are simple, low-cost, and highly recommended for the characterization of any electrode surface. In addition, the electrocatalytic usefulness of the produced AuE was tested using potassium ferrocyanide as a model electroactive analyte following the modification of the fabricated AuE surface with AuNPs.

2.0 Experimental

2.1 Chemicals and Reagents

All the solutions and analytical-grade reagents were prepared with deionized water. Potassium chloride (KCl), potassium ferrocyanide ($K_4[Fe(CN)_6]$), potassium ferricyanide ($K_3[Fe(CN)_6]$), and sodium metabisulfite ($Na_2S_2O_5$) were purchased from Sigma-Aldrich (Germany). Sulfuric acid (H_2SO_4), nitric acid (HNO_3), hydrochloric acid (HCl), and silver nitrate ($AgNO_3$) were purchased from E. Merck (Germany). The supporting electrolyte solution (0.1 M KCl) used in the electrochemical cell as electrolytic medium was prepared using analytical grade reagents not including additional purification.

2.2 Recycling of Gold from Jewellery Scrap Gold

Scrap gold (22-karat) as defective jewellery collected from the jewellery shop needs to be pre-treated prior to refinement for reducing the costs and maximizing the recycling of precious gold, which is essential to economical and efficient recovery[24]. During the pre-treatment stage, the collected scrap gold is washed and cleaned with deionized water (DIW), acidic and alkaline DIW followed by the ultrasonication to remove any dirt, adhered greasy inclusions, refractory abrasives along with other impurities on the surface of the scrap gold materials and then dried in air. The next step is established on the fact that aqua regia (a mixture of 3 parts of 37% hydrochloric and 1 part of 65% nitric acid) can dissolve gold from the pre-treated scrap gold. Consequently, the jewellery scrap gold (about 1 g) is dissolved in the aqua regia forming soluble chloride of gold with magnetic stirring to ensure full digestion of gold upon gentle heating on a water bath placed into a fume hood. After allowing the resulting mixture about 15 minutes to settle down the solid sludge impurities is filtered out by the vacuum filtration. In consequence, the solid silver chloride (AgCl) is filtered off after precipitation. At the final stage, the gold is selectively separated as precipitate from the filtrate solution by adding sodium metabisulfite (> 97%) as reducing agent. Then the gold precipitate is filtered off, washed followed by drying and thus obtained powder is melted to a solid mass (the yield was about 91%). From this bulk gold, a tablet shaped electrode (with diameter of 4 mm and thickness of 2 mm) is designed for the fabrication of AuE. There are health safety including the environmental pollution aspects that are also to be considered, during the recycling process. A brief outline of the process is presented in the Fig. 1.

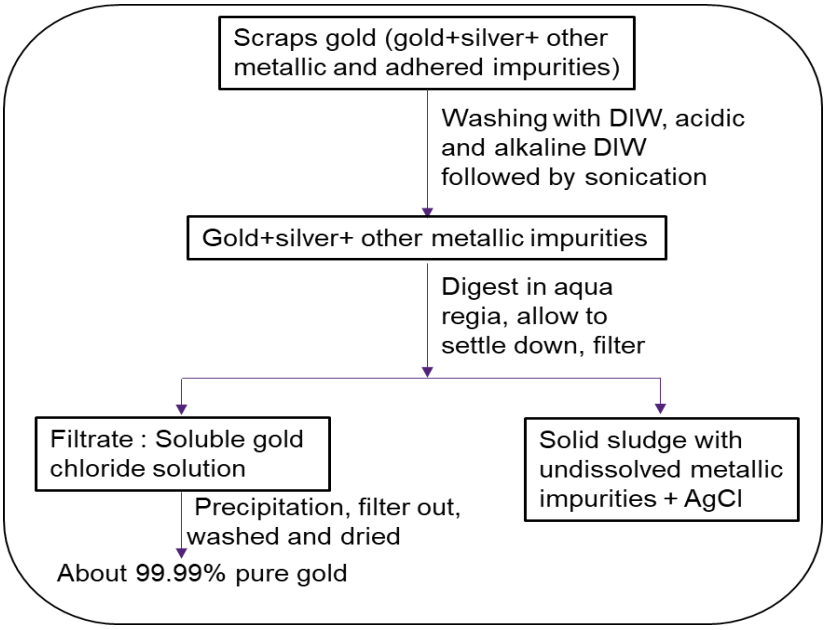

Fig.1: A outline of the recycling of gold from jewellery scrap gold.

2.3 Design of gold-Electrode and Fabrication

A schematic diagram of the fabrication process of the gold electrode (AuE) is illustrated in Fig. 2.

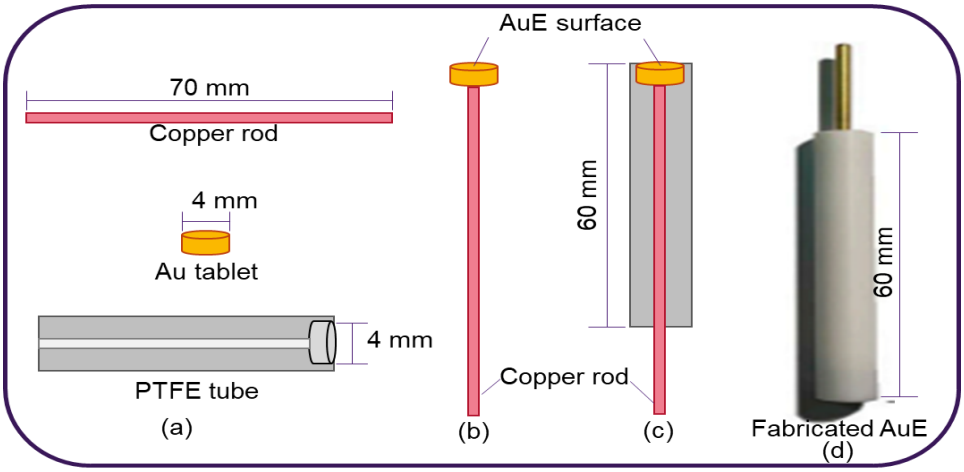

Fig. 2: Schematic diagram for the fabrication of AuE

This in-hose fabrication of the AuE is a cost-effective method, since all the electrode materials and accessories (Fig. 2a) were collected from the local market and jewellery shop. To fabricate the AuE, the recycled gold was shaped to a tablet of 4 mm diameter and 2 mm thickness, after which it was joined with a copper wire (3.5 mm diameter) as shown in Fig. 1b, to create a terminal for electrical contact. It is a simple method following which we have joined the two metals together.

Gold metal can be bonded with copper easily by heat. Copper wires have significant disadvantages compared with gold wires, since copper can oxidize at a relatively low temperature and the bonding parameters are harsher[31]. If copper wire is used, nitrogen must be used as a cover gas to prevent copper oxide formation during the bonding process. Copper is also harder than gold, which makes damage to the surface more likely. During this experiment, the two metals were joined it in an open-air environment, where we softened the gold tablet by heating and then joined with copper by quickly solidifying at room temperature to avoid the oxidation of copper. Subsequently, a polytetrafluoroethylene (PTFE) rod (6.5 mm outer diameter) was bored to fit the Cu-AuE junction rod (Fig. 1c). After fitting the Cu-AuE electrode tightly into the PTFE tube, the surface of the AuE was polished on polishing sandpaper followed by a polishing cloth to produce a mirror-like smooth surface. Then the electrode surface was washed with plenty of deionized water following sonication to clean the gold electrode surface for the electrochemical measurements and the modification with AuNPs.

2.4. AuE surface modification with gold nanoparticles (Au NPs):

Au NPs, as a standard (5 nm) Au NPs solution (Cytodiagnostics Inc, Canada) was deposited on the polished and cleaned AuE surface following the simple drop-casting method as described in the previous literatures[17, 32, 33]. In this method, 10 μL standard Au NPs solution was drop casted vertically on the AuE surface using a micropipette and then air-dried in the open air. Thus, the prepared modified electrode has been expressed as AuNP/AuE in the following texts.

2.3 Instrumentation and electrochemical measurements

Cyclic Voltammetry, Differential Pulse Voltammetry and Electrochemical Impedance Spectroscopic characterization of the fabricated AuE surface were caried out using a CHI 660E electrochemical workstation (CH Instruments, USA). The Metrohm AUTOLAB Potentiostat/Galvanostat evaluated the electrocatalytic performance of the modified AuNP/AuE surface with NOVA 2.1.4 software (METROHM, Switzerland). A 3-electrodes electrochemical cell system was used for all the electrochemical measurements, which includes the fabricated AuE (diameter of 4 mm) and modified AuNP/AuE as working electrode (WS), a platinum wire (diameter of 1 mm) as auxiliary electrode (AU), and a Ag/AgCl (KCl 3M) reference electrode (RE). The surface of the working electrode was polished with 0.05 μm alumina/water slurry (Buehler, USA) for obtaining a mirror-like finish, followed by the sonication, and then rinsed with enough distilled water before conducting the experiments. The solution system was degassed from

O_2 by purging about 30 min with N_2 gas and simultaneously stirring with a magnetic stirrer to homogenize the solution. All the electrochemical studies and characterization of the electrode surfaces were recorded with regard to the Ag/AgCl RE. The cyclic voltammetry (CV) experiments were carried out between the potential window -0.2 V and 0.8 V with 100 mVs^{-1} scan rates or otherwise specified. The experimental conditions for the DPV electrochemical measurements were as pulse period= 1000 ms, pulse amplitude = 100 mV/s, and pulse width =2 ms. The electrochemical impedance spectroscopy (EIS) measurements were conducted at the formal redox potential of $[Fe(CN)_6]^{3-}$ calculated from its cyclic voltammetric peak potentials (cathodic and anodic). The EIS spectra were recorded over a frequency range from 100 kHz to 1 Hz with an amplitude of 5 mV.

3.0 Results and discussion

The performance and characterization of the manufactured gold electrodes were performed using CV, DPV and EIS analysis at ambient temperature and pressure as discussed below.

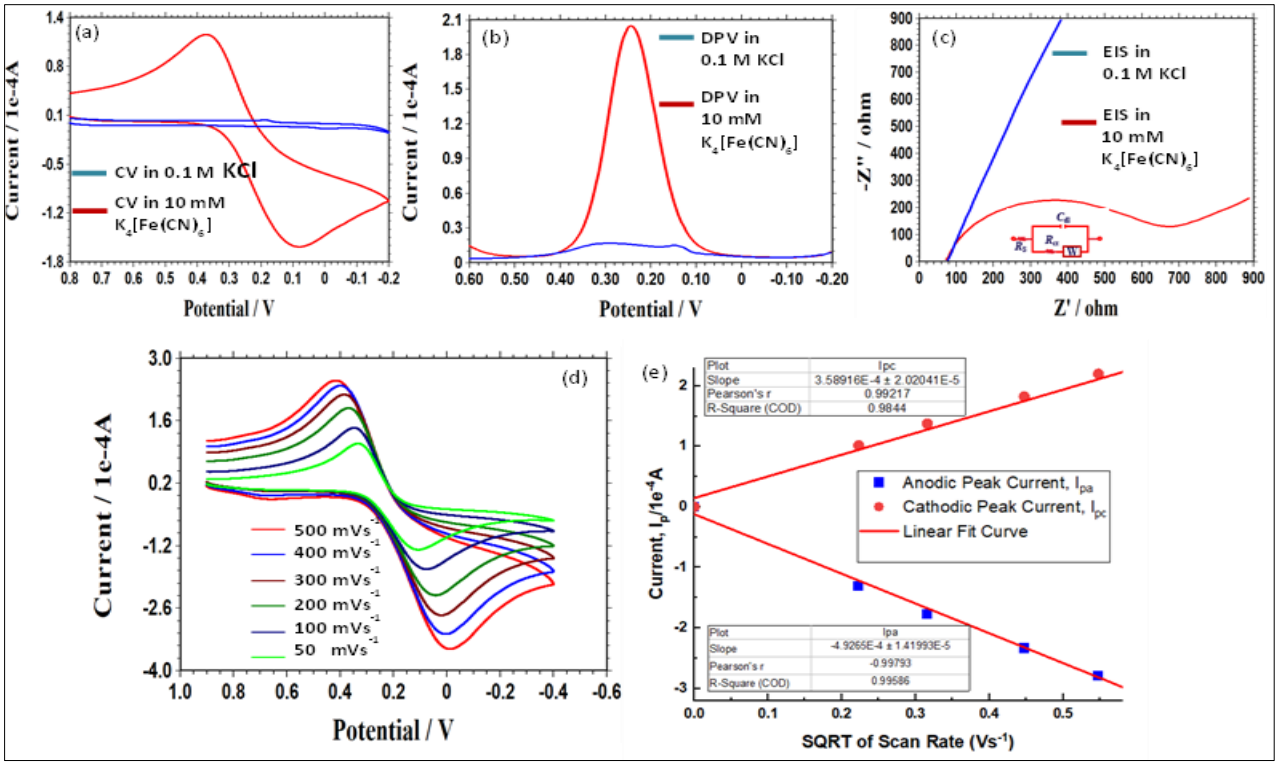

Fig. 3: Electrochemical characterization of fabricated AuE surface: comparison of (a) CV, (b) DPV and (c) EIS in 0.1 M KCl (solid line-blue) and in 10 mM $[K_3Fe(CN)_6]$ (solid line-red) at bare AuE *vs* Ag/AgCl RE at 100 mV s^{-1}, (d) The electrochemical behavior of the fabricated gold electrode surface in 10 mM $[K_3Fe(CN)_6]$ at various scan rates of 50, 100, 200, 300, 400 and 500 mV s^{-1} and (e) the corresponding Randless-Sevcick Plots: the variation of cathodic peak current(i_{pc}) and anodic peak current (i_{pa}) with SQRT of scan rate on the same electrode *vs* Ag/AgCl RE.

3.1 Cyclic Voltammetry:

Cyclic voltammogram (CV) provides information about the electrode-solution interfacial reactions occurring before and after electron transfer as well as before and after modification of the electrode surface[34-39]. This information is obtained from a comparison of peak currents between oxidation and reduction peaks which are coupled and from peak current data as a function of scan rate[40-42]. The important electrochemical parameters for a CV are the i_{pa} (anodic peak current), i_{pc} (cathodic peak current), E_{pa} (anodic peak potential) and E_{pc} (cathodic peak potential), ΔE (peak potential separation) and i_{pa}/i_{pc} (peak current ratio), etc. reveals the characteristic features of an electrode surface and its electrochemical performance. The CV measurement results obtained at the fabricated gold electrode are illustrated in Fig. 3a, d and e. Table 1 demonstrates the current-potential data, peak current ratio, and peak separation potential calculated from the voltammograms of $K_3[Fe(CN)_6]$ redox species at ambient temperature on the fabricated AuE surface *vs* Ag/AgCl RE at different scan rates (Fig. 3d). According to the CVs (Fig. 3a) taken at the bare AuE in 0.1 M KCl electrolyte (solid line-blue) and in presence of redox species (solid line-blue) *vs* Ag/AgCl at 100 mV s^{-1} scan rate between the specified potential window 0.8 V and -0.2 V, no characteristics CV peaks were found in the absence of redox species, while a pair of clearly defined redox peaks were found in presence of $K_3[Fe(CN)_6]$ at about 0.3461 V and 0.0726 V as cathodic and anodic peak, respectively. These CV data comply with the typical CV behavior of the commercial gold electrode as reported before[43, 44]. However, the validity of the Randles–Ševčík equation was also investigated for the fabricated AuE as discussed below.

In CV, the Randles–Ševčík equation represents the influence of scan rate on the peak current (i_p) that depends not only on the diffusional properties and concentration of the redox species but also on the scan rate[45, 46] as the following equation 1:

$$i_p = 0.4463\ nFAC\ (nF\ v\ D/RT)^{1/2} \quad (1)$$

Or at 25 °C[47] with the equation 2:

$$i_p = 2.69\text{x}\ 10^{-5}\ n^{3/2}\ AD^{1/2}C\ v^{1/2} \quad (2)$$

Where, i_p represents the peak current (A), n is the number of electrons transferred in the redox reaction, A denotes electrode surface area (cm^2), F is the Faraday constant (C mol^{-1}), D is the diffusion coefficient ($cm^2\ s^{-1}$), C is the concentration (mol L^{-1}), v = scan rate (Vs^{-1}), R is the Gas constant (J K^{-1} mol^{-1}), and T is temperature (K).

Table 1: Current-potential data, peak current ratio, and peak separation potential calculated from the voltammograms of $K_3[Fe(CN)_6]$ at ambient temperature on fabricated gold electrode surface vs Ag/AgCl RE

Scan rate, v (Vs^{-1})	**log v (-)**	**SQRT of Scan rate, $v^{1/2}$**	**Conc, C (mM)**	**Cath^c peak poten^l, E_{pc} (V)**	**Cath^c peak current, i_{pc} (A)x 10^4**	**Anod^c Peak Poten^l, E_{pa} (V)**	**Anod^c peak current, i_{pa} (A)x 10^4 (-)**	**Peak current Ratio, i_{pa}/i_{pc}**	**Peak separation potential, $\Delta E = (E_{pc}-E_{pa})$ (V)**	**Formal Poten^l, $E_o = (E_{pc}+E_{pa})/2$ (V)**	**Over Poten^l, η (E_{pc}- E_o) (V) (-)**
0.050	1.3	0.2236	10	0.3325	1.115	0.1042	1.315	1.18	0.2283	0.218	0.114
0.100	1.0	0.3162	10	0.3461	1.466	0.0726	1.773	1.20	0.2735	0.209	0.137
0.200	0.7	0.4472	10	0.3679	1.893	0.0353	2.338	1.23	0.3326	0.210	0.158
0.300	0.5	0.5477	10	0.3856	2.199	0.0176	2.796	1.27	0.368	0.202	0.184
0.400	0.4	0.6324	10	0.3995	2.397	0.0018	3.224	1.34	0.3977	0.201	0.199
0.500	0.3	0.7071	10	0.4191	2.519	-0.0140	3.544	1.40	0.4331	0.202	0.217

Square root = SQRT, Conc = Concentration, Cath^c= Cathodic, Poten^l = Potential, Anod^c = Anodic, RE = Reference electrode

According to the Randles–Ševčík (RS) equation the voltammograms at various scan rates display the peak current of both the anodic (i_{pa}) and cathodic ($i_{pc)}$ peaks rise when the scan rate increases (Table 1), indicating the interfacial charge transfer with diffusion on the fabricated AuE surface. Following the plot of peak current i_p (A) *vs*. SQRT of v for the AuE (as depicted in Fig. 3e) also shows that the i_p, values increase linearly (with R^2 values as 0.9844 and 0.9958 for the cathodic and anodic RS plot, respectively) with the increase of SQRT of scan rate which reveals that the electrode reaction controlled by the mass transport[33]. However, since the peak potential separation at different scan rates is found as higher than 118 mV (Table 2) the Tafel equation can be expressed as follows:

$$i = i_o\, e^{(-\alpha\, n\, F\, \eta / R\, T)} \qquad (3)$$

$$\text{or } \ln i = \ln i_o - \alpha\, n\, F\, \eta / R\, T \qquad (4)$$

where, the Tafel slope = $\alpha\, n\, F / R\, T$, α = transfer coefficient or symmetry factor (0 to 1), η = over potential

According to the calculated date depicted in Table 1 it is noticed that the overpotential η increases with the increase of v (*vs*. Ag/AgCl) which imply that the Tafel plot slope would not be zero indicates the redox process is not purely reversible. The data also reveals that the values of E_{pa} is shifted towards the negative potential and that of E_{pc} to the positive potential for increasing the

scan rate. The calculated cathodic over potentials at different scan rates show an increasing trend (Table 1) may be due to the shifting of cathodic peaks with the increase of scan rates [48]. The magnitudes of peak current ratios also explain that the electron transfer process is a quasi-reversible heterogeneous charge transfer process instead of purely reversible process. That means, the current or the rate of reaction in this quasi-reversible process is controlled by both the mass and charge transfer process. This approach holds the benefit of being pertinent to electrode reactions are not completely irreversible, in another word, those in which both the processes (anodic and cathodic) subsidize significantly to the measured currents within the overpotential window where the mass transfer properties are unimportant. This type of system is referred as *quasireversible* because the opposite charge-transfer processes be required to be considered, still a perceptible activation overpotential is mandatory to operate a certain net current across the electrode-solution interface. Therefore, the experimental data obtained for the fabricated AuE after CV analysis of $K_3[Fe(CN)_6]$ redox species demonstrate a typical cyclic voltammetric behavior that would also be applicable for the analysis of other electroactive analytes.

3.2 Differential Pulse Voltammetry (DPV)

DPV holds the advantages of lower background current and higher sensitivity regarding electrochemical response as compared to the CV. Comparing with the CV (as shown in Fig. 3a) it is also found that the DPV (as illustrated in Fig. 3b) obtained for the AuE surface shows a low background current (solid-blue line) and higher sensitivity (solid-red line) than the corresponding CV. A symmetric and well-define DPV peak at about 250 mV vs Ag/AgCl clearly indicates a stable homogeneous surface of fabricated AuE, fit for the electrochemical analysis of other electroactive species. However, in absence of redox species (Fig. 3b solid-blue line) between the Faradaic potential window, a negligible Faradaic current was observed, which also provides strong evidence against the purity of recycled gold material from the jewellery scrap gold following the aqua regia process. After a keen analysis of both the CV and DPV graph obtained at AuE in 0.1 M KCl solution (solid-blue line) it is clear that there is a tiny peak within the Faradaic region, may be due to the presence of trace amount of unknown impurity, which can be ignored considering the lowest limit of the significant response calculated from the signal-to-noise ratio.

3.3 Electrochemical Impedance Spectroscopy (EIS)

To characterize the fabricated gold electrode surface, the electrochemical charge transfer properties of the surfaces have been examined by EIS as illustrated in Fig. 3c, where the solid blue-line represents the EIS spectra as Nyquist plots at the bare AuE in 0.1 M KCl electrolyte in absence of redox species, while the solid red-curve illustrates the same plots at the same electrode surface but in presence of redox analytes, $[Fe(CN)_6]^{3-/4-}$. The EIS analysis data clearly indicates that the fabricated electrode is satisfactorily competent to response the redox species through the heterogeneous charge transfer process. The semicircle diameter of EIS (solid line-red) equals the electron transfer resistance (R_{ct}), which controls the electrode kinetics and contains information on the electron transfer kinetics of the redox species at the electrode-solution interface [17, 49]. A simplified electrical equivalent circuit consisted of the solution resistance (R_s), charge transfer resistance (R_{ct}), and electrochemical double layer capacitance (C_{dl}) has been shown at the inset of the Fig. 3c, which also comply with all the characteristic features of a typical EIS spectra for the electroactive analyte.

3.4 Electrocatalytic performance

In order to evaluate the electrocatalytic activity of the fabricated electrode (AuE) the electrochemical measurements were conducted after modification of the bare AuE surface with Au NPs and taking into consideration the response towards the $[Fe(CN)_6]^{4-/3-}$ redox couples. The investigation results and experimental data have been summarized in Fig. 4a, b, c and Table 2. The comparative CV curves (as shown in Fig. 4a) illustrate that the modified AuNP/AuE shows electrocatalytic behavior in presence of redox species with dominating electrocatalytic reduction over the electrocatalytic oxidation

Moreover, the corresponding DPV curves (Fig. 4b) also corroborated with the CV data, but the electrocatalytic sensitivity in DPV was significantly more than the CV, may be due to the inherent limitation of CV technique over DPV regarding the sensitivity. The similar DPV peak position after and before the modification of AuE surface also supports the high purity of the fabricated AuE with homogeneous surface structure. The heterogeneous charge transfer rate constant (k_o) for both bare AuE and modified AuNP/AuE has been calculated using the following equation:

$$i_o = nFAk_oC^* \quad (2)$$

where, n = the number of electrons transferred, F = the Faraday constant (96,584 C mol^{-1}), R = the gas constant (8.314 j mol^{-1} K^{-1}), T = the reaction temperature (298 K), i_o = the standard

exchange current (A) = (i_{pc} -i_{pa}), A = the geometric surface area of the electrode (0.1256 cm^2), k_o = the heterogeneous charge transfer rate constant (cm s^{-1}), and C* = the concentration of [$K_4Fe(CN)_6$] solution (0.01M).

Table 2: Current-potential data, peak current ratio, and peak separation potential calculated from the voltammograms of $K_4[Fe(CN)_6]$ at ambient temperature on Au NPs modified fabricated gold electrode surface vs Ag/AgCl RE

Scan rate, v (Vs^{-1})	log *v* (-)	SQRT of Scan rate, $v^{1/2}$	Conc, C (mM)	Cath^c peak poten^l, E_{pc} (V)	Cath^c peak current, i_{pc} (A)x 10^4 (-)	Anod^c Peak Poten^l, E_{pa} (V)	Anod^c Peak current, i_{pa} (A)x 10^4	Peak current Ratio, i_{pa}/i_{pc}	Peak separation potential, $\Delta E = (E_{pa}-E_{pc})$ (V)	Formal Poten^l, $E_o = (E_{pc}+E_{pa})/2$ (V)	Over Poten^l, η (E_{pc}-E_o) (mV) (-)
0.050	1.3	0.2236	10	0.2492	1.2728	0.3664	1.8670	1.46	0.1172	0.3078	0.0586
0.100	1.0	0.3162	10	0.2419	1.8176	0.3737	2.5952	1.42	0.1318	0.3078	0.0659
0.200	0.7	0.4472	10	0.2296	2.4802	0.3883	3.5449	1.43	0.1587	0.3089	0.0793
0.300	0.5	0.5477	10	0.2199	2.9642	0.3981	4.2425	1.43	0.1782	0.3090	0.0891
0.400	0.4	0.6324	10	0.2149	3.3560	0.4054	4.8178	1.43	0.1905	0.3101	0.0952
0.500	0.3	0.7071	10	0.2125	3.6895	0.4142	5.3527	1.45	0.2017	0.3133	0.1008

Square root = SQRT, Conc = Concentration, Cath^c= Cathodic, Poten^l = Potential, Anod^c = Anodic, RE = Reference electrode

The values of i_o for the bare AuE and modified AuNP/AuE were calculate as 3.239 $x10^{-4}$ A and 4.4128$x10^{-4}$ A, and the corresponding k_o values were found as 2.67 $x10^{-6}$ and 3.64 $x10^{-6}$ cm $s^{-1,}$ respectively. The larger values of i_o and k_o for the Au NPs modified fabricated gold electrode in comparison with the bare AuE strongly supports the electrocatalytic activity caused by the conducting high surface area Au NPs amplified the electron transfer rate of the [$K_4Fe(CN)_6$] redox species through the electrode-solution interface. In order to verify the stability of the modified electrode surface, a series of CVs were run at different scan rates between the wider choice of scan rates starting from 50 mVs^{-1} to 500 mVs^{-1} as demonstrated in Fig. 4c, which shows a stable modified electrode surface. The tabulated electrochemical data as depicted in Table 2 for the modified electrode also shows excellent consistency in terms of the ratio of peak currents (i_{pa}/i_{pc}), peak separation potential (ΔE), formal potential (E_o) and over potential (η) at different scan rates if we compare with the data (Table 1) obtained from the corresponding bare gold electrode. The peak current ratio remains almost constant at around 1.4366$\pm$0.0105, which implies quasireversible electron-transfer process like the bare AuE. An increasing trend in peak separation potential (from

0.1172 V to 0.2017 V) was also found in the modified gold electrode (like bare AuE), increasing scan rates from 50 mVs^{-1} to 500 mVs^{-1}, respectively. The formal potential obtained for the AuNP/AuE was found as 0.3095±0.0066V, which is higher than the bare electrode, while a lower trend was revealed in overpotential values (58.5 mV to 100.8 mV) throughout the same scan rates, may be due to the electrode surface modification with Au NPs. The significantly lower values of over potential at various scan rates after modification clearly indicate the electrocatalytic activity of the modified gold electrode surface [50]. Moreover, the R-S plot for the modified AuNP/AuE (as shown in the inset of Fig. 4c) at the same different scan rates satisfies the validity of the R-S equation for the modified electrode because with the increase of charging current both the oxidation and reduction peak current increases linearly as the rate of diffusion increase [33, 40].

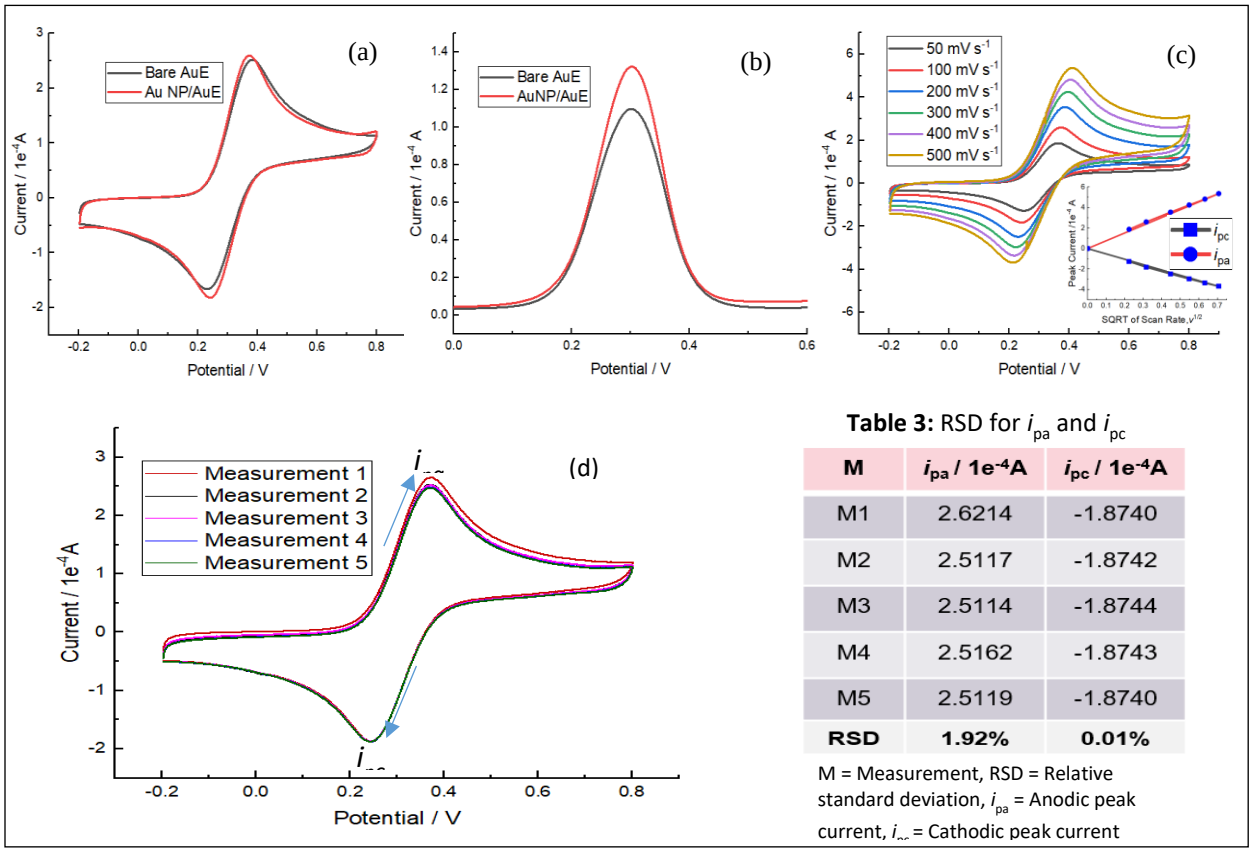

Table 3: RSD for i_{pa} and i_{pc}

M	i_{pa} / 1e-4A	i_{pc} / 1e-4A
M1	2.6214	-1.8740
M2	2.5117	-1.8742
M3	2.5114	-1.8744
M4	2.5162	-1.8743
M5	2.5119	-1.8740
RSD	**1.92%**	**0.01%**

M = Measurement, RSD = Relative standard deviation, i_{pa} = Anodic peak current, i_{pc} = Cathodic peak current

Fig. 4: Electrocatalytic performance of fabricated gold electrode surface after modification with AuNPs: comparison of (a) CV and (b) DPV in 10 mM $[K_4Fe(CN)_6]$ at fabricated bare AuE (solid line-black) and AuNPs modified AuE(solid line-red) vs Ag/AgCl reference electrode (RE) at 100 mV s^{-1}, (c) the effect of scan rate (mVs^{-1}) on the cathodic and anodic peak current ((i_{pa} and i_{pa}, respectively) including the corresponding Randless-Sevcick Plots: the variation of cathodic peak current and anodic peak current with SQRT of scan rate on the same electrode (AuNP/AuE) *vs* Ag/AgCl RE, (d) the reproducibility of the AuNPs modified fabricated gold electrode surface for the consecutive 5 measurements in 10 mM $[K_4Fe(CN)_6]$ at scan rate 100 mVs^{-1}.

Furthermore, to check the reproducibility of the modified AuNPs/AuE electrode, we have conducted 5 consecutive CV measurements in presence of redox analytes as illustrated in Fig. 4d. We also calculated the RSD (%) values for both the i_{pa} and i_{pc} as tabulated in Table 3. The RSD for i_{pc} and i_{pa} was found as 0.01% and 1.92%, respectively, which is highly satisfactory to build electrochemical sensors devices using the fabricated AuE.

4. Conclusions

The aqua regia process for recovering gold from jewellery scrap gold is a suitable, simple, and low-cost method. The cost of the fabricated gold electrode developed from recycled gold would be many times (about 20 times) lower than the commercial gold electrode. The CV, DPV and EIS electrochemical studies of the fabricated gold electrodes (both bare and modified) shows the quasi-reversible heterogeneous charge transfer reaction through the electrode-solution interface in the presence of redox species. The interfacial electron transfer rate constant is calculated as 2.67 $x10^{-6}$ and 3.64 $x10^{-6}$ cm s^{-1} for the bare and modified electrode, respectfully, which reveals the electrocatalytic behavior of the modified electrode in presence of the $[Fe(CN)_6]^{4-/3-}$ redox species. The modified electrode surface also displayed excellent reproducibility (RSD of less than 2%) to the electroactive species. The analysis data associated with the CV, DPV and EIS characterization for the fabricated gold electrode surface infer that the established AuE from recycled gold satisfies all the requirements of a typical gold electrode. The electrochemical performance studies of the modified gold electrode surface also confer the suitability of the fabricated electrode for the development of electrochemical sensors devices. The drawback during the fabrication of gold electrode is the use of N_2 gas to be maintained at the fabrication of the copper-gold junction upon heating to prevent the oxidation of copper at high temperature. Moreover, the use of high-grade scrap gold would be relatively expensive as compared to the recycling of gold from low-grade gold resources such as electronic wastage. Therefore, those drawbacks will be overcome in our future work with low-grade scrap gold. However, this investigation would introduce a platform for electrochemists (especially those from the least developed countries), who cannot afford to buy the highly expensive commercially available gold electrode from the market. This research knowledge would provide them an alternative way to fabricate a less expensive gold electrode to overcome the research barriers associated with their routine electroanalysis.

Conflicts of interest

The authors declare no conflicts of interest.

Acknowledgment

This work was supported by the NANOCAT RU grant (*RU003-2021*), Universiti Malaya. The authors also extend their gratitude to the Bangabandhu Science and Technology Fellowship Program 2021, Government of the People's Republic of Bangladesh for providing the financial support.

References

1. M. H. Naveen, R. Khan, and J. H. Bang, "Gold Nanoclusters as Electrocatalysts: Atomic Level Understanding from Fundamentals to Applications," *Chemistry of Materials,* vol. 33, no. 19, pp. 7595-7612, 2021.

2. L. Ilieva *et al.*, "Gold catalysts supported on Y-modified ceria for CO-free hydrogen production via PROX," *Applied Catalysis B: Environmental,* vol. 188, pp. 154-168, 2016.

3. A. Hashem *et al.*, "Nucleic acid-based electrochemical biosensors for rapid clinical diagnosis: Advances, challenges, and opportunities," *Critical reviews in clinical laboratory sciences,* pp. 1-22, 2021.

4. M. Al Mamun, Y. A. Wahab, M. M. Hossain, A. Hashem, and M. R. Johan, "Electrochemical Biosensors with Aptamer Recognition Layer for the Diagnosis of Pathogenic Bacteria: Barriers to Commercialization and Remediation," *TrAC Trends in Analytical Chemistry*, vol. 145, p. 116458, 2021.

5. A. Hashem, M. M. Hossain, M. Al Mamun, K. Simarani, and M. R. Johan, "Nanomaterials based electrochemical nucleic acid biosensors for environmental monitoring: A review," *Applied Surface Science Advances,* vol. 4, p. 100064, 2021.

6. S. A. Carabineiro, "Supported gold nanoparticles as catalysts for the oxidation of alcohols and alkanes," *Frontiers in Chemistry,* p. 702, 2019.

7. J. Zhao and R. Jin, "Heterogeneous catalysis by gold and gold-based bimetal nanoclusters," *Nano Today,* vol. 18, pp. 86-102, 2018.

8. M. A. Hossain, B. Paul, K. Khan, M. Paul, M. Mamun, and M. E. Quayum, "Green synthesis and characterization of silver nanoparticles by using Bryophyllum pinnatum and the evaluation of its power generation activities on bio-electrochemical cell," *Materials Chemistry and Physics,* vol. 282, p. 125943, 2022.

9. S. Zeng, K.-T. Yong, I. Roy, X.-Q. Dinh, X. Yu, and F. Luan, "A review on functionalized gold nanoparticles for biosensing applications," *Plasmonics,* vol. 6, no. 3, pp. 491-506, 2011.

10. H. Chen, X. Kou, Z. Yang, W. Ni, and J. Wang, "Shape-and size-dependent refractive index sensitivity of gold nanoparticles," *Langmuir,* vol. 24, no. 10, pp. 5233-5237, 2008.

11. K.-S. Lee and M. A. El-Sayed, "Gold and silver nanoparticles in sensing and imaging:

sensitivity of plasmon response to size, shape, and metal composition," *The Journal of Physical Chemistry B,* vol. 110, no. 39, pp. 19220-19225, 2006.

12. M. A. M. H. Abu Hashem, Ab Rahman Marlinda, Mohammad Al Mamun, Suresh Sagadevan, Zohreh Shahnavaz, Khanom Simarani and Mohd Rafie Johan, "Nucleic acid-based electrochemical biosensors for rapid clinical diagnosis: Advances, challenges, and opportunities," *CRITICAL REVIEWS IN CLINICAL LABORATORY SCIENCES,* vol. 59, no. 3, pp. 156-177, 2021.

13. M. I. Khan *et al.*, "Recent Progress in Nanostructured Smart Drug Delivery Systems for Cancer Therapy: A Review," *ACS Applied Bio Materials,* vol. 5, no. 3, pp. 971-1012, 2022.

14. X. Cao, Y. Ye, and S. Liu, "Gold nanoparticle-based signal amplification for biosensing," *Analytical biochemistry,* vol. 417, no. 1, pp. 1-16, 2011.

15. J. Wang, "Nanomaterial-based amplified transduction of biomolecular interactions," *small,* vol. 1, no. 11, pp. 1036-1043, 2005.

16. L. Nie, F. Liu, P. Ma, and X. Xiao, "Applications of gold nanoparticles in optical biosensors," *Journal of Biomedical Nanotechnology,* vol. 10, no. 10, pp. 2700-2721, 2014.

17. A. Ahammad, A. Al Mamun, T. Akter, M. Mamun, S. Faraezi, and F. Monira, "Enzyme-free impedimetric glucose sensor based on gold nanoparticles/polyaniline composite film," *Journal of Solid State Electrochemistry,* vol. 20, no. 7, pp. 1933-1939, 2016.

18. J. S. del Río, O. Y. Henry, P. Jolly, and D. E. Ingber, "An antifouling coating that enables affinity-based electrochemical biosensing in complex biological fluids," *Nature nanotechnology,* vol. 14, no. 12, pp. 1143-1149, 2019.

19. A. M. Downs *et al.*, "Nanoporous gold for the miniaturization of in vivo electrochemical aptamer-based sensors," *ACS sensors,* vol. 6, no. 6, pp. 2299-2306, 2021.

20. X. Liu, Y. Zhao, Y. Ding, J. Wang, and J. Liu, "Stabilization of Gold Nanoparticles by Hairpin DNA and Implications for Label-Free Colorimetric Biosensors," *Langmuir,* 2022.

21. V. Gude, "Microbial fuel cells as a platform technology for sustainable wastewater treatment," *Progress and Recent Trends in Microbial Fuel Cells,* pp. 375-398, 2018.

22. B. Fritz, C. Aichele, and M. Schmidt, "Environmental impact of high-value gold scrap recycling," *The international journal of life cycle assessment,* vol. 25, no. 10, pp. 1930-1941, 2020.

23. A. Hewitt, T. Keel, M. Tauber, and T. Le-Fiedler, "The ups and downs of gold recycling: understanding market drivers and industry challenges," *World Gold Council, The Boston Consulting Group,* 2015.

24. C. W. Corti, "Recovery and refining of gold jewellery scraps and wastes," in *The Santa Fe Symposium on Jewelry Manufacturing Technology,* 2002, pp. 1-20.

25. S. Syed, "Recovery of gold from secondary sources—A review," *Hydrometallurgy,* vol. 115, pp. 30-51, 2012.

26. M. W. George, "Minerals Yearbook Gold," *Reston: US Geological Survey,* 2015.

27. T. Liu, M. Li, and Q. Li, "Electroanalysis of dopamine at a gold electrode modified with N-acetylcysteine self-assembled monolayer," *Talanta,* vol. 63, no. 4, pp. 1053-1059, 2004.

28. L. Angnes, E. M. Richter, M. A. Augelli, and G. H. Kume, "Gold electrodes from recordable CDs," *Analytical chemistry,* vol. 72, no. 21, pp. 5503-5506, 2000.

29. V. B. Nascimento, M. A. Augelli, J. J. Pedrotti, I. G. Gutz, and L. Angnes, "Arrays of gold microelectrodes made from split integrated circuit chips," *Electroanalysis,* vol. 9, no. 4, pp. 335-339, 1997.

30. M. S. F. Santos, W. A. Ameku, I. G. R. Gutz, and T. R. L. C. Paixão, "Gold leaf: From gilding to the fabrication of disposable, wearable and low-cost electrodes," *Talanta,* vol. 179, pp. 507-511, 2018.

31. J.-J. Huang, H.-C. Kuo, and S.-C. Shen, *Nitride Semiconductor Light-Emitting Diodes (LEDs): Materials, Technologies, and Applications*. Woodhead Publishing, 2017.

32. A. S. Ahammad *et al.*, "Cost-effective electrochemical sensor based on carbon nanotube modified-pencil electrode for the simultaneous determination of hydroquinone and catechol," *Journal of The Electrochemical Society,* vol. 165, no. 9, p. B390, 2018.

33. M. Mamun and A. S. Ahammad, "Characterization of Carboxylated-SWCNT Based Potentiometric DNA Sensors by Electrochemical Technique and Comparison with Potentiometric Performance," *Journal of Biosensors & Bioelectronics,* vol. 5, no. 3, p. 1, 2014.

34. M. Noel and K. Vasu, "Cyclic Voítammetry and the Frontiers of Electrochemistry," *Aspect Pubi. Ltd., London,* p. 223, 1990.

35. S. Faraezi *et al.*, "Sensitivity Control of Hydroquinone and Catechol at Poly (Brilliant Cresyl Blue)-Modified GCE by Varying Activation Conditions of the GCE: An Experimental and Computational Study," *ChemEngineering,* vol. 6, no. 2, p. 27, 2022.

36. K. L. Rahman, M. Mamun, and M. Ehsan, "Preparation of metal Niacin complexes and characterization using spectroscopic and electrochemical techniques," *Russian Journal of Inorganic Chemistry,* vol. 56, no. 9, pp. 1436-1442, 2011.

37. G. J. Islam, H. N. Akhtar, M. Mamun, and M. Ehsan, "Investigations on the redox behaviour of manganese in manganese (II)–saccharin and manganese (II)–saccharin–1, 10-phenanthroline complexes," *Journal of Saudi Chemical Society,* vol. 13, no. 2, pp. 177-183, 2009.

38. M. E. Hossain, M. M. Hasan, M. Al-Mamun, and M. Q. Ehsan, "Study of interaction between Zinc (II) and aspartic acid using cyclic voltammetry," *Pakistan Journal of Scientific & Industrial Research Series A: Physical Sciences,* vol. 55, no. 2, pp. 72-79, 2012.

39. M. Laiju, H. N. Akhtar, M. Mamun, M. A. Jabbar, and M. Ehsan, "Cyclic voltammetric study on the effect of the introduction of secondary ligands on the redox behaviour of the copper-saccharin complex," *Journal of the National Science Foundation of Sri Lanka*, vol. 38, no. 2, 2010.

40. M. Mamun, O. Ahmed, P. Bakshi, and M. Ehsan, "Synthesis and spectroscopic, magnetic and cyclic voltammetric characterization of some metal complexes of methionine:[(C5H10NO2S) 2MII]; MII= Mn (II), Co (II), Ni (II), Cu (II), Zn (II), Cd (II) and Hg (II)," *Journal of Saudi Chemical Society*, vol. 14, no. 1, pp. 23-31, 2010.

41. M. Mamun, O. Ahmed, P. Bakshi, S. Yamauchi, and M. Ehsan, "Synthesis and characterization of some metal complexes of cystine:[Mn (C6H10N2O4S2)]; where MII= Mn (II), Co (II), Ni (II), Cu (II), Zn (II), Cd (II), Hg (II) and Pb (II)," *Russian Journal of Inorganic Chemistry*, vol. 56, no. 12, pp. 1972-1980, 2011.

42. M. M. Hasan, M. E. Hossain, M. Mamun, and M. Ehsan, "Study of redox behavior of Cd (II) and interaction of Cd (II) with proline in the aqueous medium using cyclic voltammetry," *Journal of Saudi Chemical Society*, vol. 16, no. 2, pp. 145-151, 2012.

43. S. Moulton, J. Barisci, A. Bath, R. Stella, and G. Wallace, "Investigation of protein adsorption and electrochemical behavior at a gold electrode," *Journal of colloid and interface science*, vol. 261, no. 2, pp. 312-319, 2003.

44. S. Bollo, C. Yánez, J. Sturm, L. Nunez-Vergara, and J. A. Squella, "Cyclic voltammetric and scanning electrochemical microscopic study of thiolated β-cyclodextrin adsorbed on a gold electrode," *Langmuir*, vol. 19, no. 8, pp. 3365-3370, 2003.

45. A. A. Gewirth, "Inorganic Electrochemistry: Theory, Practice and Application By Piero Zanello (University of Siena, Italy). Royal Society of Chemistry: Cambridge. 2003. xiv+ 616 pp. $199.00. ISBN 0-85404-661-5," ed: ACS Publications, 2004.

46. H. N. Akhtar and M. Ehsan, "Electrochemical Comparative Studies On The Redox Behavior Of Cu (II) And Cr (II) Before And After Interactions With Ciprofloxacin In Solutions," *International Academic Journal of Applied Bio-Medical Sciences*, vol. 2, no. 5, 2021.

47. A. J. Bard and L. R. Faulkner, *Student Solutions Manual to accompany Electrochemical Methods: Fundamentals and Applicaitons, 2e*. John Wiley & Sons, 2002.

48. L. Xiong, D. Lowinsohn, K. R. Ward, and R. G. Compton, "Fabrication of disposable gold macrodisc and platinum microband electrodes for use in room-temperature ionic liquids," *Analyst*, vol. 138, no. 18, pp. 5444-5452, 2013.

49. P. Hashemi, A. Afkhami, H. Bagheri, S. Amidi, and T. Madrakian, "Fabrication of a novel impedimetric sensor based on l-Cysteine/Cu (II) modified gold electrode for sensitive determination of ampyra," *Analytica chimica acta*, vol. 984, pp. 185-192, 2017.

50. A. u. H. A. Shah, S. Zia, G. Rahman, and S. Bilal, "Performance Improvement of Gold Electrode towards Methanol Electrooxidation in Akaline Medium: Enhanced Current Density

Achieved with Poly (aniline-co-2-hydroxyaniline) Coating at Low Overpotential," *Polymers,* vol. 14, no. 2, p. 305, 2022.